Available online at www.CivileJournal.org

Civil Engineering Journal

Vol. 5, No. 3, March, 2019

Finite Element Modelling of RC T-Beams Reinforced Internally with GFRP Reinforcements

Balamuralikrishnan R. [a*], Saravanan J. [b]

[a] *Asst. professor, Department of BNE, College of Engineering, National University of Science and Technology, Muscat, PO Box:2322, CPO Seeb 111, Sultanate of Oman.*

[b] *Department of Civil and Structural Engineering, Annamalai University, Pin:608001,Tamilnadu, India.*

Received 24 December 2018; Accepted 12 February 2019

Abstract

Fibre reinforced polymers (FRP) are being used extensively in the rehabilitation and retrofitting of existing structures as an external reinforcement because of their properties like high strength to weight and stiffness to weight ratios, corrosion resistance, light weight and high durability. They are especially used in the reinforced concrete structure like bridges, chimney, high rise building etc. At present FRP reinforcements are available in the form of reinforcing bars and are used in the structures in place of steel, mainly the structures are constructed near the coastal areas or in the aggressive environments. The main advantage of FRP rebar is its corrosion resistance, light weight, durability and easy handing. The FRP rebars are being used worldwide for many structures including bridge structures as well, but not well explored because of its availability. The main objective of this thesis work is to assess the static load behaviour of RC T-beams reinforced internally with GFRP reinforcements using finite element analysis software ANSYS. Totally twelve numbers of specimens were considered in this study with varying parameters such as type of reinforcements, reinforcements ratio and concrete grade. Modelling of the T- beams were done with ANSYS using solid 65 and link 8 element and the same were analyzed under static loading conditions. The results obtained from the ANSYS were compared with the theoretical and experimental analysis. Based on the comparison suitable conclusions and recommendations are made in this research work.

Keywords: Highway Black Spots; Speed Study; Warning; Satisfaction; Affectability.

1. Introduction

Concrete structure reinforced with conventional steel reinforcements cause a concern in aggressive environmental conditions due to accelerating problem of corrosion. The down fall results in costly maintenance or replacement of the existing structure. Glass Fibre Reinforcement Polymer (GFRP) bars is becoming the wave of the future due to their resistance to corrosion, high strength to weight ratios and the ability to handle the material with such simplicity. Glass Fibre - reinforced polymers (GFRP) are non - metallic reinforcement utilizing high performance hybrid, the surfaces of the rods are treated with undulations to provide mechanical interlock with concrete. Their application is seen primarily as a means to avoid corrosion problems encountered in concrete structures when using conventional steel as reinforcements. Keeping this in mind, the present research was planned to study the behaviour of GFRP reinforcements for beam - column applications.

* Corresponding author: balamuralikrishnan@nu.edu.om

http://dx.doi.org/10.28991/cej-2019-03091268

1.2. Fibre Reinforced Polymer

FRP composite is defined as a polymer matrix, whether thermosetting (e.g., polyester, vinyl ester, epoxy, phenolic) or thermoplastic (e.g., nylon, PET) which is reinforced by fibre (e.g., aramid, carbon, glass). Specific definition used within the report also include glass fibre reinforced polymer (GFRP), carbon fibre reinforced polymer (CFRP) and related abbreviation. FRP material is currently used as reinforced for concrete structure in which corrosion protection is a primary concern. FRP material is corrosion resistant and exhibit several properties that make suitable as structural reinforcement.

Now a days, all these fibres under tensile loading exhibit a linear elastic behaviour up to failure [1, 2, 3] without showing yielding. Carbon and aramid fibres are anisotropic with different values of mechanical and thermal properties in the main directions whereas glass fibres are isotropic materials in nature [4, 5]. Glass fibres are transparent to radio frequency radiation and are used in radar antenna applications [6]. Reinforcement materials can be designed with unique fibre architectures and are preformed or shaped depending on the product requirements and manufacturing process. Some of the FRP reinforcements that are commercially available in different forms. Carbon fibres, stress corrosion is not a problem. But as graphite conducts electrical current when makes contact with steel, it may result in galvanic corrosion problems. Carbon fibres possess a negative or very low [coefficient of thermal expansion in their longitudinal direction and have an excellent dimensional stability [7]. Resistance to higher temperature is low for aramid fibres as compared to glass and carbon fibres. Aramid fibres also possess high tensile stress over a long period of time [8]. Thermoplastics are polymers, which do not develop cross-links.

They are capable of being reshaped and repeatedly softened and hardened when exposed to some temperature values above their forming temperature. Thermosetting resins are easy for processing and low in cost. The most common thermosetting resins are epoxy, polyesters, vinyl ester, etc. Epoxy resins are prepared by the ring opening polymerization of compounds containing an average of more than one epoxy group per molecule. The main advantages of epoxy resins are good mechanical properties, easy processing and lower shrinkage during curing which lead to good bond characteristics.

Moreover epoxy resins have a wide range of stiffness. Polyester matrices are made by using ethylene glycol with either orthophthalic or isophtalic acid as the saturated diacid and numeric as the unsaturated diacid. Polyester resins have good UV resistance and are used in outdoor applications especially where corrosion resistance is required. Vinyl ester matrices are resins based on methacrylate and acrylate and are more flexible a have higher fracture toughness, good wet out and good adhesion with glass fibres. It has the combination of all the good properties of epoxy resins and polyesters and make them preferred choice in the production of glass fibre reinforced composites. Besides, vinyl ester resins are highly resistant to acids, alkalis, solvents and peroxides.

The flexural behaviour of concrete filled steel tube beams under two point loading system and results are verified with the finite element analysis using ANSYS in the FE model. The FE analysis result and EC4 standard codes show that the experimental investigation of yield conservative prediction behaviour of CFTS beams [9]. The finite element analysis of steel and laminated composite rail way tie under static and dynamic loads for the FEA analysis of steel and laminated composite tie[10]. In hybrid GFRP/steel reinforced concrete beams, the steel reinforcement improved the beam stiffness, ductility and load resistance after cracking. The higher the amount of GFRP reinforcement, the less the rate of increase of the ultimate capacity of the concrete beam [11].

Hybrid GFRP-steel reinforced concrete beams had good bond performance when installing the GFRP bars as near as possible to the outer surface of the concrete element, which is beneficial in term of structural performance of the reinforcing bars [12]. The deflection of FRP beams significantly decreased compared to reinforced concrete beams while the ultimate loads were increased [13]. The behavior of concrete beams were strengthened with GFRP unidirectional composite laminates behaves better than the RCC beam [14].

The ANSYS16.2 FEA models are more effective to analyze reinforced concrete beams in combination with steel and GFRP bars and the results obtained from FEA are very close to results observed in the experiments [15,16]. The steel bars increased the ductility of hybrid GFRP-steel reinforced concrete beams [17]. Compared with conventional RC beams, concrete beams reinforced with steel-FRP stirrups successfully showed a considerable increase in the beam shear strength and deformability [18].

1.2. Types of FRP Reinforcements

FRP rods are a typical product produced by the pultrusion process. A secondary process occurs to add surface deformations if required for adequate bond properties. Geometrical shape and surface texture can also be manipulated. A helical fibre over-winding, protruding ribs, or a sand coating can be added to the smooth outer layer of resin. FRP reinforcing bars are available as smooth, braided, spiral wound, sand coated and as a twisted rod strand. While these surface characteristics are beneficial, one must be aware that by simply increasing bar diameter can decrease its ultimate strength.

In reduced cross-sections, increasing fiber volume can increase strength properties. The various types of FRP reinforcements available in the market are shown in Figure1. Steel and FRP rods samples in this study is shown in Figure 2 and different sizes of FRP reinforcement bars are shown in Figure 3.

The objectives and scope of this present study is,

- To determine the mechanical properties of concrete, steel and GFRP reinforcements.
- To analyze the results obtained from the experiments of the T-beam reinforced with GFRP reinforcement.
- To model the RC-T beams using ANSYS 12 [19].
- Finite elements analysis will be carried out only using ANSYS 12.

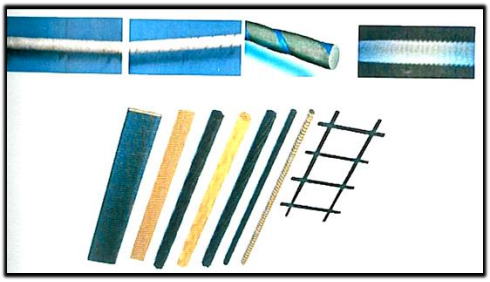

Figure 1. Various types of FRP reinforcement

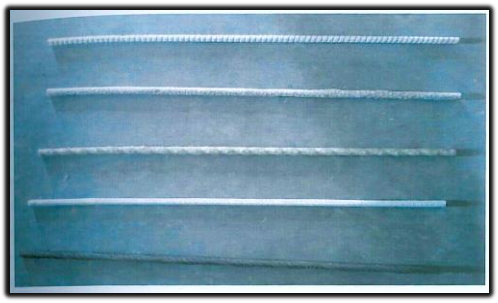

Figure 2. Steel and FRP rods samples rod in the study

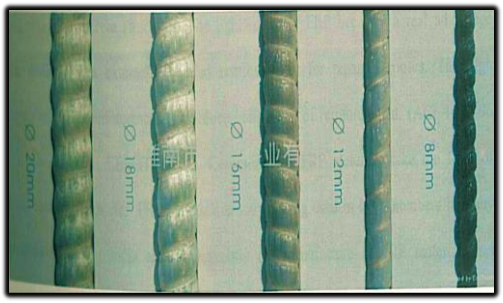

Figure 3. Different sizes of FRP reinforcement bars

2. Theoretical Analysis

2.1. Test specimens

Totally twelve number of test specimens were cast by considering three different reinforcement ratios, two different grades of concrete in each category. Of which three of them are control specimens reinforced with conventional steel bars and other three are reinforced with GFRP bars (balanced, under and over reinforced). The specimens were designed and reinforced in such way that under, balanced and over reinforced flanged concrete beam. The specimen consists flange of size 450 × 75 mm and web of 125 × 175 mm reinforced with conventional steel and the length of the beam is 3200 mm. Main reinforcements of flanged beam were made up of high yield strength deformed steel bars of 12 mm diameter for control specimens and GFRP bars of same diameters used for GFRP specimens.

The reinforcement for under reinforced, balanced and over reinforced beams with 2 Nos. of 12 mm diameter at top and bottom, 2 Nos. of 12 mm diameter at top and 3 Nos. of 12mm diameter at bottom, 2 Nos. of 12 mm diameter at top and 5 Nos. of 12mm diameter at bottom respectively. Stirrups 8mm diameter at 150 mm c/c. The same quantity of conventional reinforcement replaced with GFRP bars including stirrups. For better bonding the GFRP bars are made with threaded surface. The reinforcement details are shown in Fig. 4, 5 and 6.

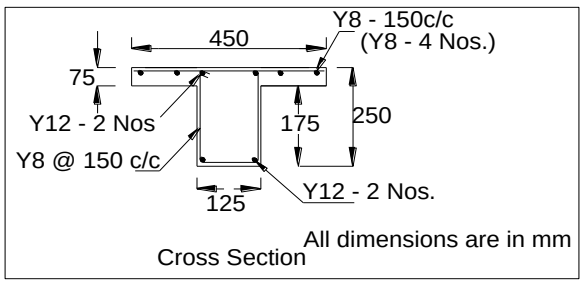

Figure 4. Cross section of under reinforced flanged beam

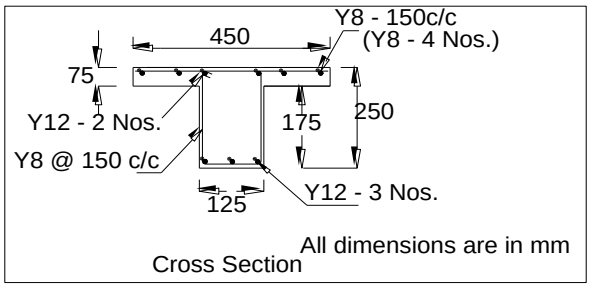

Figure 5. Cross section of balanced flanged beam

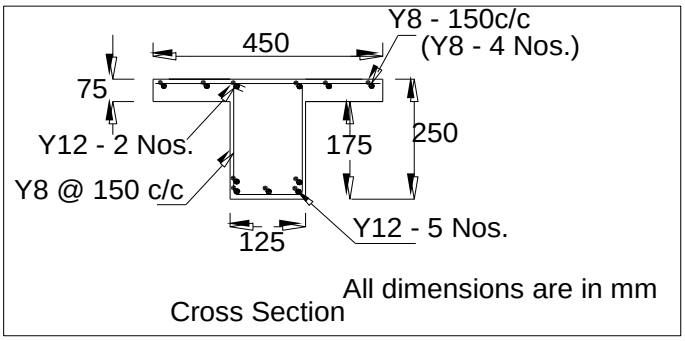

Figure 6. Cross section of over reinforced flanged beam

2.2. Reinforcement Ratio Details

Table 1 shows the number of the test specimens for the analysis was derived based on the varying parameters considered in the study.

Table 1. Details of the test specimens

Reinforcement	Grade of concrete M20				Grade of concrete M30			
	ρ1	ρ2	ρ3	Total	ρ1	ρ2	ρ3	Total
Steel	1	1	1	3	1	1	1	3
GFRP	1	1	1	3	1	1	1	3
Total	12 Beams							

ρ1 - Bottom Two Rod, ρ2 - Bottom Three Rod, ρ3 - Bottom Five Rod.

2.3. Theoretical Moment Curvature Relationship for T-Beam (Figure 7)

The analytical moment curvature for a reinforced section can be determined under the following assumptions

- Perfect bond between concrete and reinforcement
- Plane and sections remain plane under loading
- Simplifications of the stress-strain relationship for the constituent materials

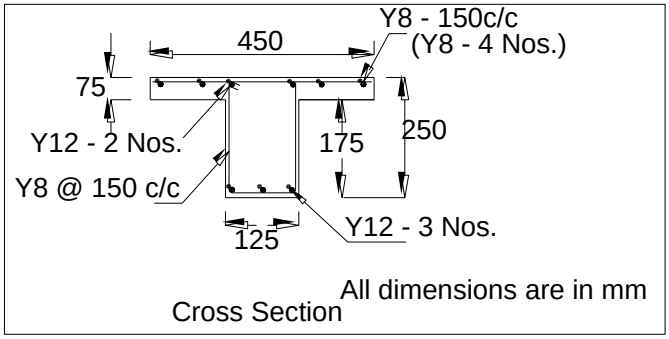

Figure 7. Cross section of flanged concrete beam

2.4. Theoretical Calculation Result

Theoretical results were calculated for all the cases say $Bm_1F_e\rho_1$, $Bm_1F_e\rho_2$, $Bm_1F_e\rho_3$, $Bm_2F_e\rho_1$, $Bm_2F_e\rho_2$, $Bm_2F_e\rho_3$, $Bm_1F_T\rho_1$, $Bm_1F_T\rho_2$, $Bm_1F_T\rho_3$, $Bm_2F_T\rho_1$, $Bm_2F_T\rho_2$, and Bm2FTρ3. The theoretical results for sample results one in each case are presented in Table 2 to 5.

Table 2. Theoretical value for $Bm_1F_e\rho_1$

M_{cr} (Nmm)	$\emptyset_{cr}$ (rad/mm)	Load (N)	Deflection (mm)
0	0	0	0
448514.04	8.57E-07	0.896	0.934427
2143416.12	1E-06	40.86	13.798
20428158.6	1.3E-05	147.7	27.03
73857224.4	2.33E-05	191.1	31.014

Table 3. Theoretical value for $Bm_2F_e\rho_1$

M_{cr} (Nmm)	$\emptyset_{cr}$ (rad/mm)	Load (N)	Deflection (mm)
0	0	0	0
554737.442	8.57E 07	1.1094	0.9345
2518763.33	1.01E 06	41.366	12.82
20683403.9	1.17E 05	215.282	26.05
107641356	2.24E-05	292.18	30.42

Table 4. Theoretical value for $Bm_1F_T\rho 1$

M_{cr} (Nmm)	$\emptyset_{cr}$ (rad/mm)	Load (N)	Deflection (mm)
0	0	0	0
438310.05	8.57E 07	0.87662	0.934427
1760828.13	1.03E 06	176.72	44.895
88368004.4	4.15E 05	192.9	50.402
96455691.4	4.7E 05	199.18	51.507

Table 5. Theoretical values for $Bm_2FT\rho 1$

M_{cr} (Nmm)	$\emptyset_{cr}$ (rad/mm)	Load (N)	Deflection (mm)
544531.211	8.57E 07	0	0
2151663.16	1.03E 06	1.088	0.934565
136884385	4.15E 05	273.76	45.37511
149412427	4.7E 05	298.82	50.805
154270082	4.98E 05	308.54	51.91

2.5. Theoretical Result

The values obtained from the theoretical analysis for all the cases are produced in the form of moment - curvature and load - deflection curves. For sample of few cases only are shown in Figures 8 and 9.

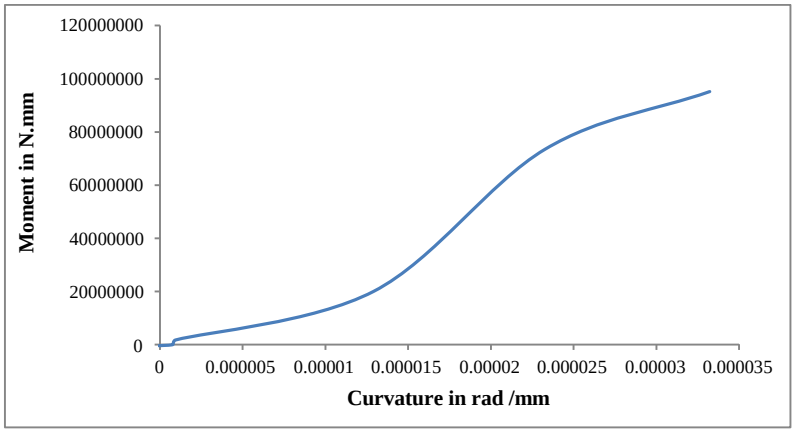

Figure 8. M-Φ curve for specimen $Bm_1F_e\rho_1$

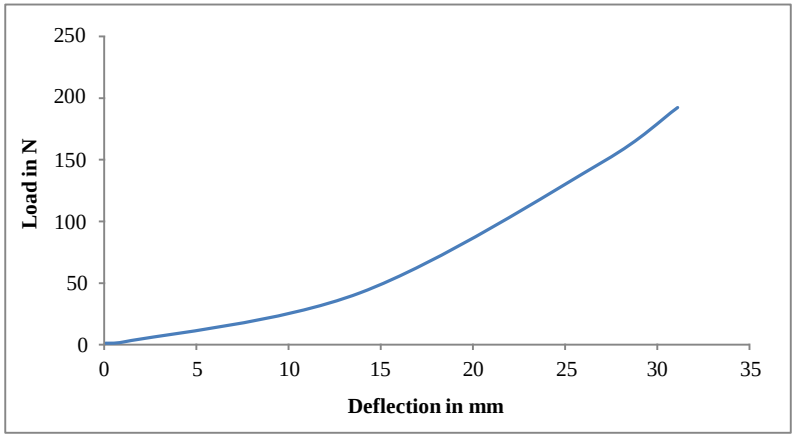

Figure 9. Load - deflection for specimen $B_{m1}F_e\rho_1$

3. Finite Element Modeling

3.1. Compressive Behaviour of Concrete

The nonlinear response of concrete is inelastic. The concrete stress-strain relation exhibits nearly linear elastic response up to about 30% of the compressive strength. This is followed by gradual softening up to the concrete compressive strength, when the material stiffness drops to zero. Beyond the compressive strength the concrete stress-strain relation exhibits strain softening until failure takes place by crushing.

3.2. Tensile Behaviour of Concrete

In this study, the file behaviour is assumed as an elastic brittle process and the cracks are formed in the direction of tensile force after concrete strength reduces abruptly to zero. In his paper, it has not been not interested in the tensile strength of concrete, but the influence of the cracked concrete zone on the structural behaviour. A simplified averaging procedure, which figures that cracks are distributed across a region of the finite element. In this model, cracked concrete is supposed to remain continuum and the material properties are the modified to account for the damage induced in the material. After the first crack has occurred, the concrete becomes orthotropic with the material directions of cracking.

3.3. Behaviour FRP Reinforcements in Tension

Glass fibre reinforcement FRP bars, the most common commercially available from a number of manufactures. These bars are either a sand coated external layer, a moulded a deformation layer, to create a bond between concrete and FRP surface. FRP bars are typically elastic and brittle. Such that a stress strain relation in axial tension is linear elastic to failure. Ductile steel like failure does not occur and hence it is fundamentally different from conventional steel [20].

3.4. Finite Element Software (ANSYS 2012)

ANSYS a suite of powerful engineering simulation programs, based on the finite element method, which can solve problems ranging from relatively simple linear analyses to the most challenging nonlinear simulations. In a nonlinear analysis ANSYS automatically chooses appropriate load increments and convergence tolerances. The description and properties of the modelling elements are studied in this Phase.

3.5. Properties of Materials

3.5.1. Tensile Strength

FRB bars are anisotropic, with the longitudinal axis being the strong axis. The mechanical properties of FRP composites vary significantly from one product to another. Factors such as volume and type of fiber and resin, fiber orientation, dimensional effects, and during manufacture, play a major role in establishing product characteristics. The stress-strain curve for HYSD bars and FRP rebar are found out by carrying tension test experimentally and the curves are shown in Figures 10 (a) to (c).

FRP bars and tendons reach their ultimate tensile strength without exhibiting any material yielding. The mechanical properties of FRP reported here are measured in the longitudinal (i.e. strong) direction. The tensile strength of FRP bars is a function of bar diameter. This phenomenon results in reduced strength and efficiency in larger diameter bars. For example, for GFRP reinforcement produced by one U.S. manufacturer the tensile strength ranges from nearly 480 MPa for 28.7 mm bars to 890 MPa for 9.5 mm bars.

(a)

(b)

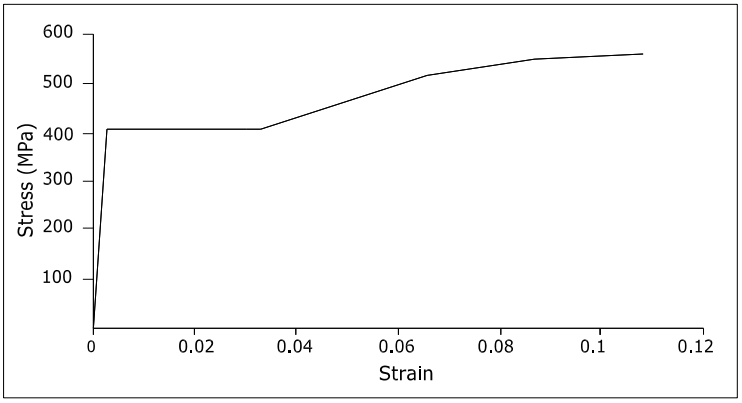

(c)

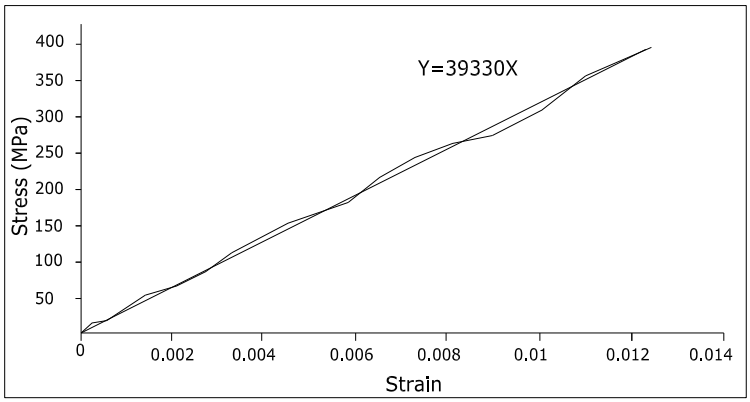

Figure 10. (a) Tensile testing of GFRP reinforcements, (b) Stress -Strain curve for HYSD bar, (c) Stress-Strain curve for GFRP rods

3.5.2. Specific Gravity

FRP bars have a specific gravity ranging from 1.5 to 2.0 as they are nearly four times lighter than steel. The reduced weight leads to lower transportation and storage costs and decreased handling and installation time on the job site as compared to steel reinforcing bars. This is an advantage that should be included in ANSYS analysis for product selection.

3.5.3. Thermal Expansion

Reinforced concrete itself is a composite material, where the reinforcement acts as the strengthening medium and the concrete as the matrix. It is therefore imperative that behaviour under thermal stresses for the two materials be similar so that the differential deformations of concrete and the reinforcement are minimized. Depending on mix proportions, the linear coefficient of thermal expansion for concrete varies from 6 to 11 × 10^{-6} /°C (4 to 6 × 10^{-6}/ °F) are the coefficients of thermal expansion for typical FRP rebars 9.9×10^{-6} per C (5.5×10^{-6}/°F).

3.5.4. Tensile Elastic Modulus

The longitudinal modulus of elasticity of GFRP bars is approximately 25 percent that of steel. The modulus for GFRP bars found from the stress-strain obtained from the tension test as similar to the steel bars. The elastic modulus of GFRP rebars were found that it ranges from 0.4 to 0.6 x 10^5 MPa.

3.4.5. Fatigue

FRP bars exhibit good fatigue resistance. Most research in this regard "has been on high-modulus fibers (e.g., aramid and carbon), which were subjected to large cycles of tension-tension loading in aerospace applications. In tests where the loading was repeated for 10 million cycles, it was concluded that carbon-epoxy composites have better fatigue strength than steel, while the fatigue strength of glass composites is lower than steel at a low stress ratio.

3.6. Modelling Basics

3.6.1. Element Types

The element types for this model are shown in Table 14. The Solid65 element was used to model the concrete. This element has eight nodes with three degrees of freedom at each node translations in the nodal x, y, and z directions. This element is capable of plastic deformation, cracking in three orthogonal directions, and crushing. A schematic of element is shown in Figure 11.

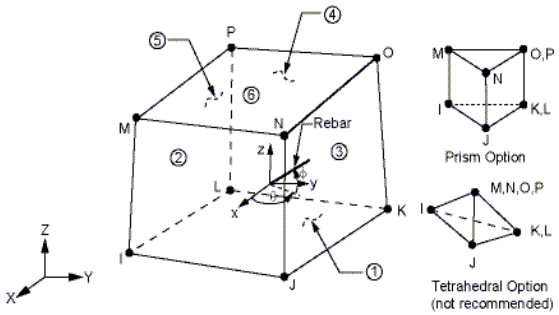

Figure 11. Solid 65 elements

Table 14. Element Types for working model

Material Type	ANSYS Element
Concrete	Solid65
GFRP	Link8
Steel Reinforcement	Link8

A Link 8 element was used to model steel reinforcement. This element is a 3D spar it and it has two nodes with three degrees of freedom - translations in the nodal x, y and z directions. This element is also capable of plastic deformation. It is shown in Figure 12.

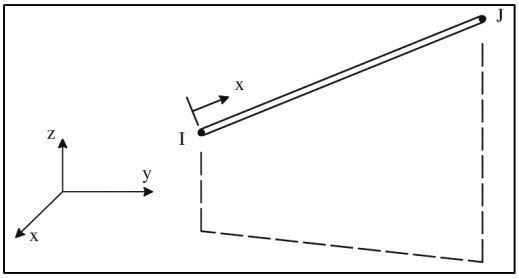

Figure 12. LINK 8 Element

3.7. Material Property

- **Beam size 250 mm × 450 mm, length 3200 mm.**
- **Material for concrete – 1, Concrete (Linear Isotropic, Concrete):**

Density = 24000 N/mm^2, E= 2.86×10^4 N/mm^2, and μ= 0.15

- **Material for GFRP – 3, GFRP (Linear Isotropic):**

Density = 1600 gr/cm^3, E = 0.47×10^5 N/mm^2, and μ= 0.30

- **Material for steel – 2, Steel (Linear Isotropic):**

Density = 7810 kgf/m^3, Yield Stress = 432 N/mm^2, E = 2.1×10^5 N/mm^2, and μ= 0.30

- **Reinforcement:**

Top: 2 Nos. – Y12

Bottom: 2, 3, 5 Nos. – Y12

Stirrups: R8@150 mm c/c

Cover: 25 mm @ top & 25 mm @ bottom

- **Element types used: Solid 65 for Concrete**
- **Link 8 for Reinforcement (Table 15)**

Table 15. Link 8 for Reinforcement

Description	Diameter of Bar (mm)	Area (m^2)
Stirrups	8	50.2655×10^{-6}
Flange Reinforcement	12	113.097 × 10^{-6}
Bottom Reinforcement	12	113.097 × 10^{-6}

- **C3D8R**

The ELEMENT option deals with the element-nodal connectivity list. The element type is specified using the TYPE parameter. The choice of element type is as important as any aspect of a finite element analysis. In this model the element used is C3D8R- 8 - node linear brick element (Figure 13). In this C response continuum, D represents displacement and H represents Hybrid.

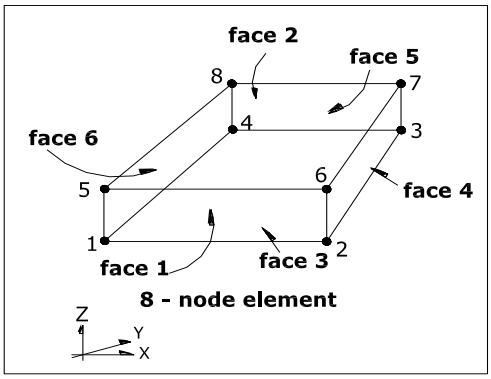

Figure 13. Continuum solid element

- **Rebar**

Rebar is used to define layers of uniaxial reinforcement in solid elements. Such layers are as a smeared layer with a constant thickness equal to the area of each reinforcing bar divided by the reinforcing bar spacing (Figure 14).

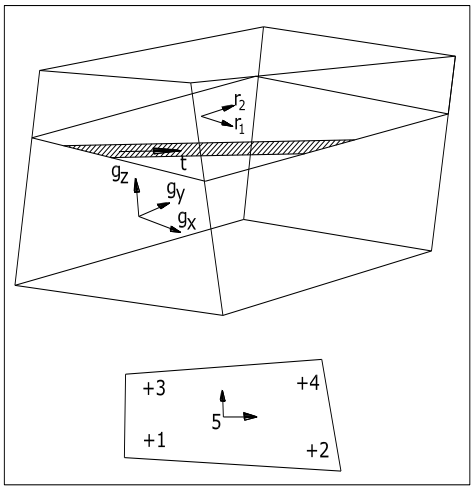

Figure 14. Rebar model in 3D element

3.8. Modelling of T-beams

In order to compare the performance of the T-beam the specimens were modelled and analyzed using a finite element software ANSYS 12 using the above said element types and the material properties are shown in Figures 15 to 20 and the deflected profile for few cases are shown in Figures 21 and 22.

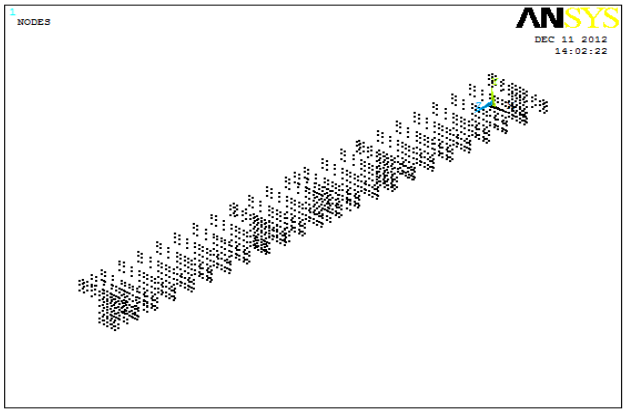

Figure 15. Nodes-ANASYS Model

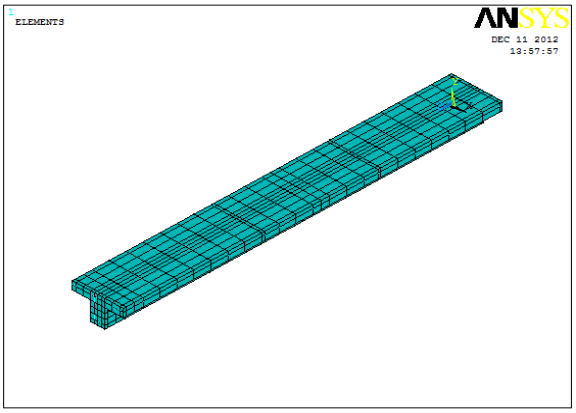

Figure 16. Solid 65 Elements for Concrete

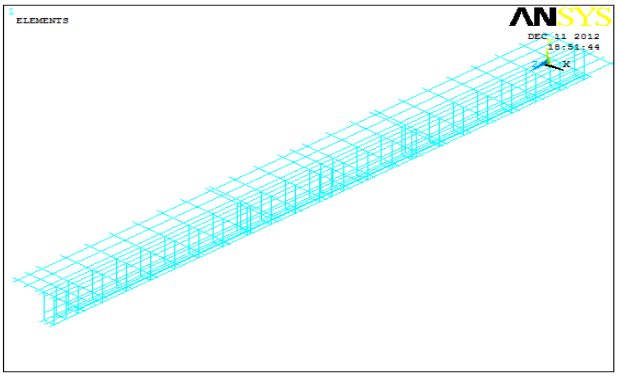

Figure 17. Link 8 Element for Reinforcements

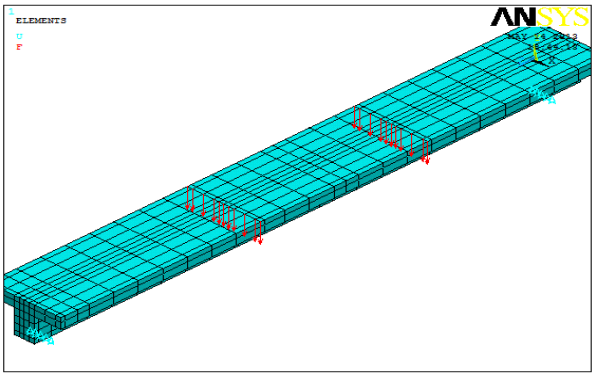

Figure 18. Model with Loading Conditions

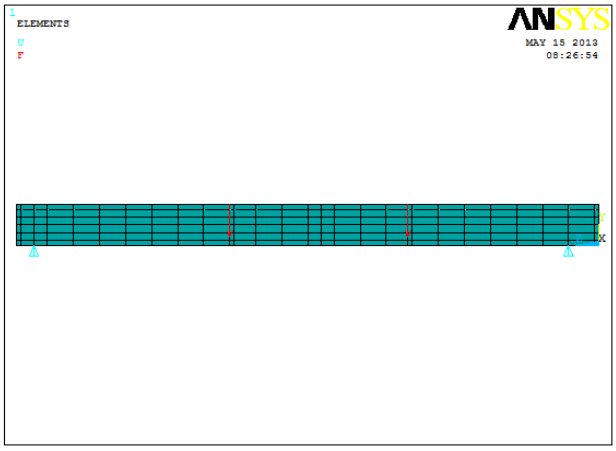

Figure 19. Model showing Support conditions

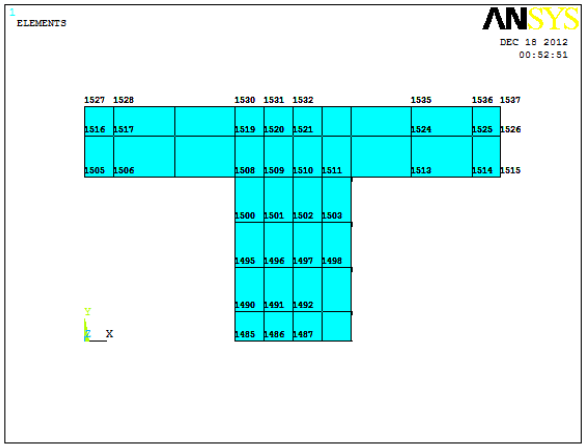

Figure 20. Cross sections of the T-beam modelling with node numbers

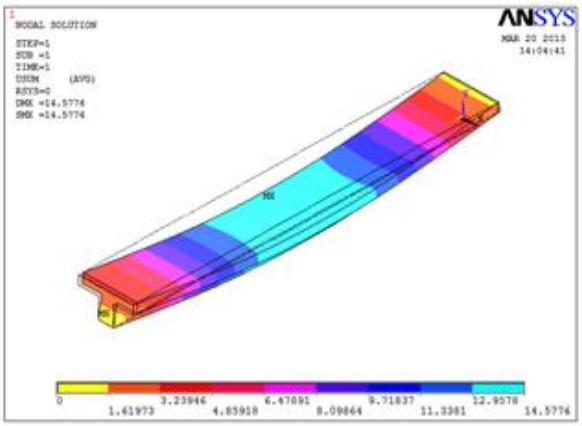

Figure 21. Typical deflected shape of the T beam reinforced with steel

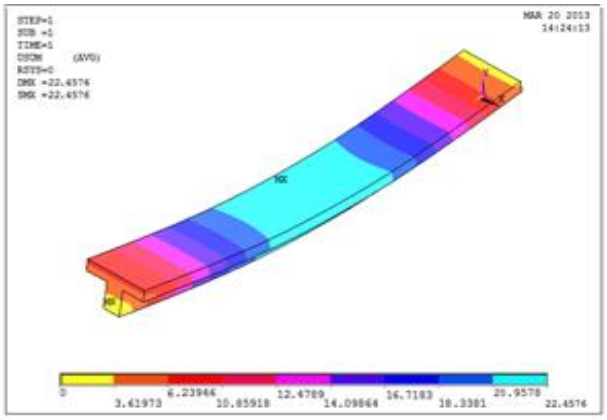

Figure 22 .Typical deflected shape of the T beam reinforced with GFRP

3.9. Results of Analytical Results (ANSYS)

The load - deflection behavior of T- beam from ANSYS results are shown in Figures 23 and 24.

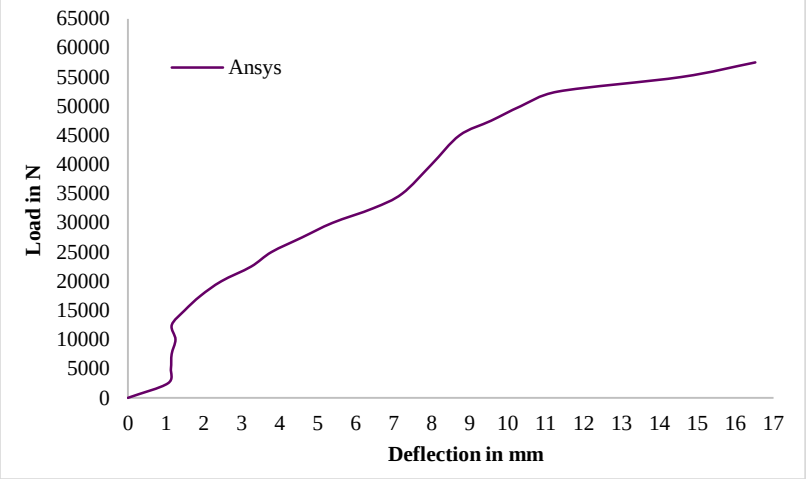

Figure 23. Load-Deflection Curve of Bm1Feρ1

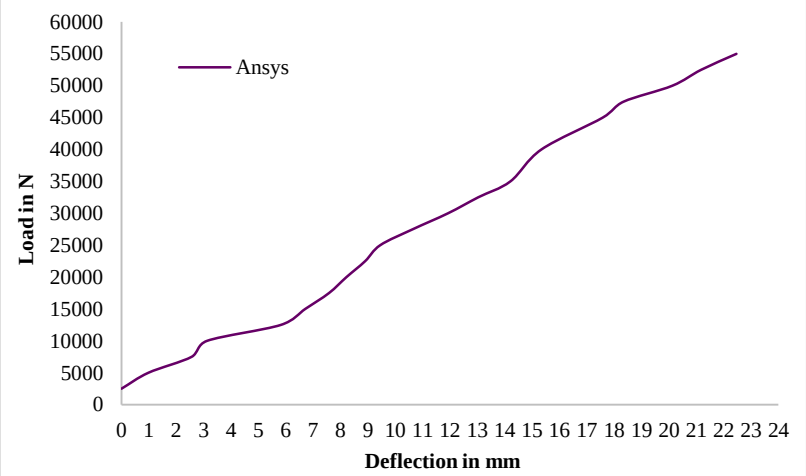

Figure 24. Load- Deflection for fiber specimen Bm1Ftρ1

4. Comparison of ANSYS Results with Experimental Results

Totally three series of specimen were cast with three different reinforcement ratio and two mix ratios. The different reinforcement ratios were (i) Two rods at the bottom (ii) Three rods at the bottom iii) Five rods at the bottom. The mix ratios were (i) M20 grade concrete (ii) M30 grade concrete. The series of the specimens were named as (i) Beam reinforced with conventional steel reinforcement (BmFeρ) ii) Beam reinforced with Grooved type GFRP reinforcements (BmFtρ). Among these series GFRP reinforced beam was high performance than the conventional steel reinforced beam. The results of the experimental study already carried out were considered for the comparison of analytical results. The analytical and experimental results are presented in the form of load – deflection graphs is shown in Figure 25.

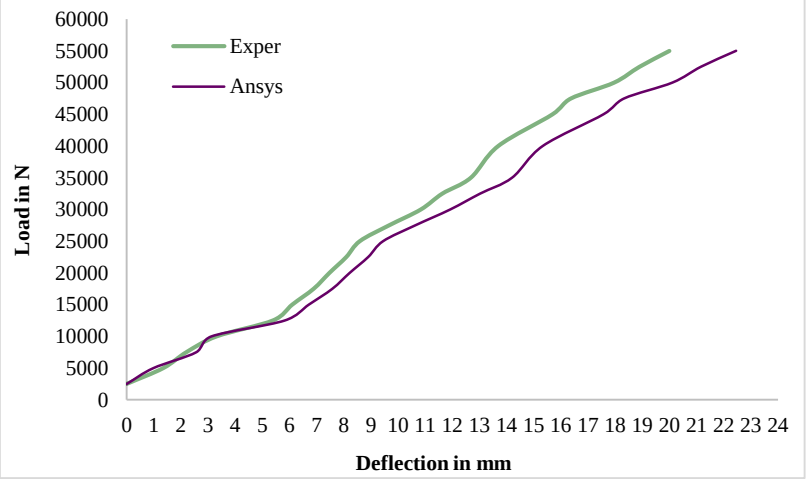

Figure 25. Load - Deflection for steel specimen Bm1Feρ1

4.1. Discussion

- From the load-deflection curves it is observed that identical results are obtained.
- Test specimens with GFRP reinforcements load carrying capacity is 5% lower than the steel reinforced specimens almost for all the test specimens.
- Increase of concrete grade is increasing the load carrying capacity of the test specimens invariably for all the specimens by 5% to 20%.
- The deflection of the higher concrete grade M30 is lower than the M20 grade by 10%
- The deflection is higher for the GFRP reinforced specimens than the steel reinforced specimens in all the cases and varies from 5% to 15%.
- Larger crack widths are observed in the experimental results but it is not so in the case of ANSYS. But numbers of cracks are more for the GFRP specimens.

5. Conclusions

Based on the experimental and numerical results the following conclusions are drawn:

- The Modulus of Elasticity of GFRP bars are lesser than that of steel bars which is experimentally observed. Since the GFRP reinforcement having lower modulus of elasticity, resulted in higher deflection than the steel reinforced specimens.
- The ultimate moment carrying capacity of the GFRP reinforced beam is higher than the conventional steel reinforced beam.
- The FRP reinforced beams exhibit a brittle behaviour before failure, as seen from stress strain curves. However the predominant failure mode is by compression of concrete.
- The load carrying capacity of the GFRP reinforced beam is almost equal with the conventional steel reinforced beam.
- The GFRP reinforced beam was higher residual deflection value than the conventional steel reinforced beam.
- The first crack developed for the conventional reinforced specimens at 3 tons whereas for the GFRP specimens crack developed at the 5 tons but the performance of the flanged beam is only 10 to 20% variation for the steel and GFRP specimen respectively.
- The experimental results of the flanged beams holds very good agreements with the analytical results for the both flanged beam reinforced with steel and GFRP reinforcements. The performance of the flanged beam predicted by the analytical tool ANSYS is almost equal to the experimental values.

6. Conflict of Interest

The authors declare no conflict of interest.

7. References

[1] El-Sayed, A.K. “Concrete Contribution to the Shear Resistance of FRP-Reinforced Concrete Beams”. Ph.D. thesis, University of Sherbrooke, Sherbrooke, Quebec, Canada (2006).

[2] El-Sayed, Ahmed, Ehab El-Salakawy, and Brahim Benmokrane. “Shear Strength of One-Way Concrete Slabs Reinforced with Fiber-Reinforced Polymer Composite Bars.” Journal of Composites for Construction 9, no. 2 (April 2005): 147–157. doi:10.1061/(asce)1090-0268(2005)9:2(147).

[3] ISIS-M03-07. “Reinforcing Concrete Structures with Fiber Reinforced Polymers”. The Canadian Network of Centers of Excellence on Intelligent Sensing for Innovative Structures, ISIS Canada, University of Winnipeg, Manitoba (2007) .

[4] ACI Committee 440. “Guide for the design and construction of concrete reinforced with FRP bars”. ACI 440.1R-06, American Concrete Institute, Farmington Hills, Michigan (2006).

[5] CAN / CSA S806 -11. Design and construction of building components with fibre reinforced polymers. Canadian Standards Association, Rexdale, Ontario (2011).

[6] El - Sayed, A.K., El - Salakawy E.F., Benmokrane, B. “Shear capacity of high-strength concrete beams reinforced with FRP bars”. ACI Structural Journal 103(3) (2006): 383-389.

[7] ACI Committee 440. Guide Test Methods for Fiber Reinforced Polymers (FRPs) for Reinforcing or Strengthening Concrete Structures, ACI 440.3R-04, American Concrete Institute, Farmington Hills, Michigan (2004).

[8] ACI Committee 318. "Building Code Requirements for Structural Concrete (318-08) and commentary (318R-08)". American Concrete Institute, Farmington Hills, Michigan (2008).

[9] Soundararajan, R., Arivalagan and Shanmugasundaram. "Finite Element Analysis on the Flexural Behaviour of Concrete Filled Steel Tube Beams". Journal of Structural Engineering 20 (1) (2010): 88-94.

[10] Gueroui, Djelailia, Badouna Baha-Eddine, and Fadel Djamel. "Landscape Approaches as a Strategic Tool in the Environmental Management of Resources and Territories: Case of Aïn Dalia Dam in Northeastern Algeria." INTERNATIONAL JOURNAL OF ADVANCED ENGINEERING AND MANAGEMENT 2, no. 5 (May 1, 2017): 118. doi:10.24999/ijoaem/02050030.

[11] Mustafa, Suzan A.A., and Hilal A. Hassan. "Behavior of Concrete Beams Reinforced with Hybrid Steel and FRP Composites." HBRC Journal 14, no. 3 (December 2018): 300–308. doi:10.1016/j.hbrcj.2017.01.001.

[12] Smring, Santa binti, Norhafizah Salleh, NoorAzlina Abdul Hamid, and Masni A. Majid. "Finite Element Modelling of Concrete Beams Reinforced with Hybrid Fiber Reinforced Bars." IOP Conference Series: Materials Science and Engineering 271 (November 2017): 012093. doi:10.1088/1757-899x/271/1/012093.

[13] Kh. Hind, M., Özakça, M., and Ekmekyapar, T. "A Review on nonlinear finite element analysis of reinforced concrete beams Retrofitted with fiber reinforced polymers". Journal of Advanced Research in Applied Mechanics 22(1) (2016): 13-48.

[14] Subramani, T., Jayalakshmi, J. "Analytical investigation of bonded glass fibre reinforced polymer sheets with reinforced concrete beam using ANSYS". International Journal of Application or Innovation in Engineering & Management (IJAIEM) 4(5) 2015: 105-112.

[15] Premalatha, J., Shanthi Vengadeshwari, R., Srihari, P. "Finite element modeling and analysis of RC beams with GFRP and steel bars". International Journal of Civil Engineering and Technology (IJCIET) 8(9) (2017): 671-679.

[16] Pathak, Prabin, and Yi Xia Zhang. "Finite Element Simulation for Nonlinear Finite Element Analysis of FRP Strengthened RC Beams with Bond-Slip Effect." Applied Mechanics and Materials 846 (July 2016): 440–445. doi:10.4028/www.scientific.net/amm.846.440.

[17] Smring, Santa binti, Norhafizah Salleh, NoorAzlina Abdul Hamid, and Masni A. Majid. "Finite Element Modelling of Concrete Beams Reinforced with Hybrid Fiber Reinforced Bars." IOP Conference Series: Materials Science and Engineering 271 (November 2017): 012093. doi:10.1088/1757-899x/271/1/012093.

[18] Fahmy, Mohamed F. M., Zainab E. Abd-ElShafy, and Zhishen Wu. "Experimental and Numerical Evaluation of the Shear Behavior of Reinforced Concrete T-Beams with Hybrid Steel-FRP Stirrups." Journal of Composites for Construction 21, no. 4 (August 2017): 04017007. doi:10.1061/(asce)cc.1943-5614.0000790.

[19] ANSYS, Ins. "ANSYS fluent 12.0 User's Guide." New Hampshire: ANSYS INC (2009).

[20] Ferreira, A.J.M, P.P Camanho, A.T Marques, and A.A Fernandes. "Modelling of Concrete Beams Reinforced with FRP Re-Bars." Composite Structures 53, no. 1 (July 2001): 107–116. doi:10.1016/s0263-8223(00)00182-3.